boundary. The proposed infinite determinant method accurately locates the lines of transition between stable and unstable regions of the parameter space, but it yields no useful information concerning the character of the solution in regions away from these boundaries.

References

[1] Floquet, G., "Sur les Equation Différentielles Linéaires à Coefficients Périodiques," *Annales de École Normal Superior*, Paris, Vol. 2, No. 12, 1883, pp. 47–89.

[2] L. Cesari, *Asymptotic Behavior and Stability Problems in Ordinary Differential Equations*, 2nd ed., Academic Press, New York, 1963, pp. 55–59.

[3] Kane, T. R. and Sobala, D. "A New Method for Attitude Stabilization," *AIAA Journal*, Vol. 1, No. 6, June 1963, pp. 1365–1367.

[4] Mingori, D. L., "The Determination By Floquet Analysis of the Effects of Energy Dissipation on the Attitude Stability of Dual-Spin Satellites," *AIAA Journal*, Vol. 7, No. 1, Jan. 1969, pp. 20–27.

[5] Bolotin, V. V., *Dynamic Stability of Elastic Systems*, Holden-Day, San Francisco, 1964.

[6] Goldstein, H., *Classical Mechanics*, Addison-Wesley, Reading, Mass., 1959, pp. 215–217.

[7] Liapunov, A. M., "Problème Général de la Stabilité du Mouvement," *Annales de la Faculte des Sciences de l'Universite de Toulouse pour les Sciences Mathematiques et les Sciences Physiques*, Vol. 2, No. 9, 1907; also *Annals of Mathematical Studies*, Vol. 17, Princeton Univ. Press, Princeton, N.J., 1949.

[8] Malkin, I. G., *Theory of Stability of Motion*, AEC-tr-3352, United States Atomic Energy Commission, pp. 217–219; translated from publication of State Publishing House of Technical-Theoretical Literature, Moscow-Leningrad, 1952.

[9] Meirovitch, L. and Wallace, F. B., Jr., "Attitude Instability Regions of a Spinning Unsymmetrical Satellite in a Circular Orbit," *Journal of the Astronautical Sciences*, Vol. 14, 1967, pp. 123–133.

[10] Likins, P. W. and Mingori, D. L., "Liapunov Stability Analysis of Spinning Systems," *Proceedings of the 18th International Astronautical Congress*, Pergamon Press, 1968, pp. 89–101.

[11] Lindh, K. G., "Analysis of the Stability of Systems of Periodic Differential Equations by an Extended Infinite Determinant Method," Ph.D. dissertation, Dec. 1968, Univ. of Calif., Los Angeles, Calif.

APRIL 1970 AIAA JOURNAL VOL. 8, NO. 4

Buckling and Postbuckling Behavior of Spherical Caps under Axisymmetric Load

JAMES R. FITCH*
General Electric Company
Schenectady, N. Y.

AND

BERNARD BUDIANSKY†
Harvard University
Cambridge, Mass.

The elastic buckling and initial postbuckling behavior of clamped shallow spherical shells under axisymmetric load is investigated. An analysis is made of the dependence of the buckling and postbuckling behavior on the area of the region over which the load is uniformly distributed. It is found that as the area of the loaded region increases, the buckling behavior changes from asymmetric bifurcation to axisymmetric snap-through, and then back to asymmetric bifurcation. The asymmetric buckling associated with a small loaded area is characterized by the fact that the shell retains its load carrying capacity. The opposite is true for the bifurcation associated with a relatively large loaded area. A simple criterion for determining whether a loss of load carrying capacity will occur is established in terms of the radius and thickness of the shell and the radius of the projection of the loaded area on the shell base plane.

Introduction

THIS paper presents an analysis of the buckling and initial postbuckling behavior of a clamped spherical cap (Fig. 1) uniformly loaded over a circular region centered at the apex. Huang[1] analyzed the buckling of this structure under uniform pressure. For the case of a concentrated load at the apex, Bushnell[2] analyzed buckling, and Fitch[3] studied the postbuckling as well as the buckling behavior. For both types of loading it was found that if the shell thickness is less than a certain critical value asymmetric bifurcation will occur at a smaller load than that required for axisymmetric snap-buckling. The initial postbuckling analysis for the concentrated load case showed that the shell retains its load carrying capacity as it makes the transition to asymmetric behavior. This result is in qualitative agreement with experiments[4–6] in which the gradual development of asymmetric deformation with increasing load has been observed. Experiments on the clamped cap under uniform pressure,[7–9] on the other hand, have shown that buckling is of the sharp snap-through variety. In this paper an analysis of the dependence

Received January 17, 1969, revision received September 25, 1969. This work was supported in part by NASA under Grant NGL 22-007-012, and by the Division of Engineering and Applied Physics, Harvard University.

* Applied Mathematics Group, Knolls Atomic Power Laboratory.

† Professor of Structural Mechanics, Division of Engineering and Applied Physics. Member AIAA.

of the buckling and postbuckling behavior on the size of the region over which the load is distributed is undertaken.

The investigation is carried out on the basis of Marguerre's nonlinear shallow shell theory.[10] Critical loads for axisymmetric snap-buckling and asymmetric bifurcation are computed numerically, the latter through a standard perturbation technique which leads to a linear eigenvalue problem. When the bifurcation load is smaller than the axisymmetric critical load an extension of the perturbation idea is used to investigate the initial postbuckling behavior.

Basic Equations

According to the nonlinear shallow shell theory of Marguerre[10] the behavior of a thin spherical cap loaded uniformly over a circular region centered at the apex (Fig. 1) can be described by the nondimensional equations

$$\nabla^4 w = \nabla^2 f + \left(\frac{1}{x} f' + \frac{1}{x^2} \ddot{f}\right) w'' + \left(\frac{1}{x} w' + \frac{1}{x^2} \ddot{w}\right) f'' - 2\left(\frac{1}{x} \dot{f}' - \frac{1}{x^2} \dot{f}\right)\left(\frac{1}{x} \dot{w}' - \frac{1}{x^2} \dot{w}\right) + 4ps(\bar{\lambda} - x) \quad (1)$$

$$\nabla^4 f = -\nabla^2 w + \left(\frac{1}{x} \dot{w}' - \frac{1}{x^2} \dot{w}\right)^2 - \left(\frac{1}{x} w' + \frac{1}{x^2} \ddot{w}\right) w'' \quad (2)$$

where x and Θ are polar coordinates in the base plane,

$$(\ )' \equiv \partial/\partial x(\ ), \ (\dot{}) \equiv \partial/\partial\Theta(\ )$$

$$\nabla^2(\ ) \equiv (\ )'' + 1/x(\ )' + 1/x^2(\ddot{})$$

and

$$s(x) = \begin{cases} 0, & x<0 \\ 1, & x>0 \end{cases}$$

The nondimensional radial coordinate x, vertical deflection w, stress function f, and pressure p are related to the corresponding physical variables by

$$x = \lambda r/r_0, \ w = (\lambda^2/2H)W, \ f = (\lambda^4/4EH^2t)F$$

$$p = \frac{q}{(32EH^3t/\lambda^2 r_0^4)} = \frac{q}{2E/[3(1-\nu^2)]^{1/2}\,(t/R)^2}$$

In these expressions, r_0, H, and t are the base radius, apex rise, and thickness of the shell (Fig. 1). E is Young's modulus,

$$\lambda = 2[3(1-\nu^2)]^{1/4}(H/t)^{1/2} = [12(1-\nu^2)]^{1/4}(r_0/t)\,(t/R)^{1/2}$$

where ν is Poisson's ratio and the relation $r_0^2 \approx 2RH$ has been used to introduce the shell radius R. The parameter $\bar{\lambda}$ in (1) is $(\bar{r}/r_0)\lambda$ where $\bar{r}$ is the radius of the projection of the loaded region on the base plane. The completely clamped condition (no displacement or rotation) at the outer edge implies

$$w = w' = 0 \quad (3, 4)$$

$$f'' - (\nu/\lambda)f' - (\nu/\lambda^2)\ddot{f} = 0 \quad (5)$$

$$\lambda\left(f'' - \frac{\nu}{x} f' - \frac{\nu}{x^2} \ddot{f}\right)' - \frac{1}{\lambda} f' - \frac{1}{\lambda^2} \ddot{f} + \nu f'' + 2(1+\nu)\left(\frac{1}{x} \ddot{f}\right)' = 0 \quad (6)$$

at $x = \lambda$. Equations (5) and (6) follow[1] from the conditions of vanishing radial and tangential displacement. The description of the problem can be completed by appropriate regularity conditions on w and f at $x = 0$.

Axisymmetric Behavior

For axisymmetric deflections (1–6) can be shown to reduce to

$$(x\theta')' - (\theta/x) + x\Phi = -2p\bar{\lambda}^2 y(x) + \theta\Phi \quad (7)$$

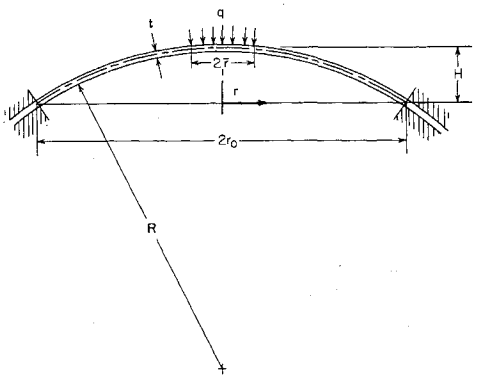

Fig. 1 Geometry of a clamped spherical cap.

$$(x\Phi')' - (\Phi/x) - x\theta = -\tfrac{1}{2}\theta^2 \quad (8)$$

$$\theta(\lambda) = 0 \quad (9)$$

$$\lambda\Phi'(\lambda) - \nu\Phi(\lambda) = 0 \quad (10)$$

where $\theta = -w'$, $\Phi = f'$, and

$$y(x) = \begin{cases} (x/\bar{\lambda})^2, & x<\bar{\lambda} \\ 1, & x>\bar{\lambda} \end{cases} \quad (11)$$

In this case the appropriate apex conditions are

$$\theta(0) = \Phi(0) = 0 \quad (12, 13)$$

which follow, respectively, from symmetry and the requirement that the membrane stresses be bounded.

Average Deflection Parameter

It will be convenient to introduce some nondimensional gross measure of the deflection of the cap under a given load. A suitable choice is the ratio of the average vertical displacement of the loaded area to the shell thickness, which is given by

$$\frac{1}{\pi\bar{r}^2 t}\int_0^{2\pi} d\Theta \int_0^{\bar{r}} rW\,dr \equiv \frac{\overline{W}}{t}$$

When W is axisymmetric it can be shown that

$$\frac{\overline{W}}{t} = \frac{1}{[12(1-\nu^2)]^{1/2}}\int_0^{\lambda} y\theta\,dx \quad (14)$$

where y is the function defined previously. The term "load deflection curve" will be used to denote a plot of p vs $\overline{W}/t$.

Buckling and Postbuckling Behavior

Buckling

The critical load for axisymmetric snap-buckling corresponds to the first local maximum on the load-deflection curve implied by Eqs. (7–13). Asymmetric bifurcation may occur before this load is reached, however, in which case the bifurcation load is critical. An analysis of the initial postbuckling behavior is then needed to complete the description of the buckling phenomenon. It is necessary to determine whether the load initially increases or decreases after bifurcation. If it decreases buckling will be of the sharp snap-through variety; if it increases the cap will make a smooth transition to asymmetric behavior.

Asymmetric bifurcation can be investigated by seeking a solution to Eqs. (1–6) in the form

$$\begin{Bmatrix} w \\ f \end{Bmatrix} = \begin{Bmatrix} \int_x^{\lambda} \theta\,dx \\ \int_0^{x} \Phi\,dx \end{Bmatrix} + \epsilon \begin{Bmatrix} w_1(x,\Theta) \\ f_1(x,\Theta) \end{Bmatrix} \quad (15)$$

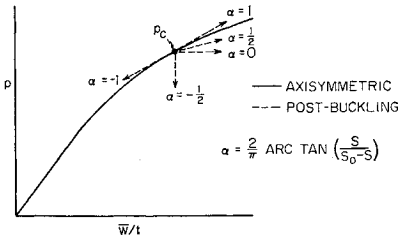

Fig. 2 Interpretation of postbuckling parameter α, defined in terms of instantaneous axisymmetric stiffness S_0 and postbuckling stiffness S.

where ϵ is an infinitesimal scalar parameter. Substitution of (15) in (1–6), use of (7–13), and linearization with respect to ϵ gives

$$\nabla^4 w_1 = \nabla^2 f_1 - \left(\frac{1}{x} f'_1 + \frac{1}{x^2}\ddot{f}_1\right)\theta' + \frac{1}{x} w''_1\Phi - \frac{1}{x} f''_1\theta + \left(\frac{1}{x} w'_1 + \frac{1}{x^2}\ddot{w}_1\right)\Phi'$$

$$\nabla^4 f_1 = -\nabla^2 w_1 + \left(\frac{1}{x} w'_1 + \frac{1}{x^2}\ddot{w}_1\right)\theta' + \frac{1}{x} w''_1\theta$$

and boundary conditions (3–6) on (w_1,f_1). With no loss of generality (w_1,f_1) may be taken in the form

$$\begin{Bmatrix} w_1 \\ f_1 \end{Bmatrix} = \begin{Bmatrix} w_{1n}(x) \\ f_{1n}(x) \end{Bmatrix} \cos n\Theta$$

which leads to the equations

$$L_n{}^2(w_{1n}) = L_n(f_{1n}) - \left(\frac{1}{x} f'_{1n} - \frac{n^2}{x^2} f_{1n}\right)\theta' + \frac{1}{x} w''_{1n}\Phi - \frac{1}{x} f''_{1n}\theta + \left(\frac{1}{x} w'_{1n} - \frac{n^2}{x^2} w_{1n}\right)\Phi' \quad (16)$$

$$L_n{}^2(f_{1n}) = -L_n(w_{1n}) + \left(\frac{1}{x} w'_{1n} - \frac{n^2}{x^2} w_{1n}\right)\theta' + \frac{1}{x} w''_{1n}\theta \quad (17)$$

$$w_{1n}(\lambda) = w'_{1n}(\lambda) = 0 \quad (18, 19)$$

$$f''_{1n}(\lambda) - \frac{\nu}{\lambda} f'_{1n}(\lambda) + \frac{n^2\nu}{\lambda^2} f_{1n}(\lambda) = 0 \quad (20)$$

$$\lambda f''_{1n}(\lambda) - \frac{1}{\lambda}[1 - \nu + (2+\nu)n^2] f'_{1n}(\lambda) + \frac{3n^2}{\lambda^2} f_{1n}(\lambda) = 0 \quad (21)$$

where

$$L_n(\ ) \equiv (\ )'' + \frac{1}{x}(\ )' - \frac{n^2}{x^2}(\ ) \text{ and } L_n{}^2(\ ) = L_n L_n(\ )$$

The critical load for bifurcation buckling may now be described as the smallest value of p for which (16–21) have a nontrivial solution for any integer n.

Initial Postbuckling Behavior

Koiter[11,12] originated a theory of initial postbuckling behavior which leads, via an asymptotically exact calculation, to a determination of whether the load initially increases or decreases after buckling. This result can then be used to predict the buckling behavior of the same structure when it has an initial geometric imperfection. It can be shown that if the load decreases after buckling for the perfect structure the corresponding imperfect structure would be expected to buckle at a load below the classical critical load. The application of this theory to a spherical cap was developed in some detail in Ref. 3 and only a brief outline will be presented here.

We begin by making the assumption that immediately after bifurcation the solution to Eqs. (1–6) may be written in the form

$$\begin{Bmatrix} w \\ f \end{Bmatrix} = \begin{Bmatrix} \int_x^\lambda \theta\, dx \\ \int_0^x \Phi\, dx \end{Bmatrix} + \epsilon\begin{Bmatrix} w_1 \\ f_1 \end{Bmatrix} + \epsilon^2\begin{Bmatrix} w_2 \\ f_2 \end{Bmatrix} + \ldots \quad (22)$$

where (θ,Φ) is the solution to the axisymmetric problem at the given load, and the buckling mode (w_1,f_1) has been normalized such that the maximum value of $W_1(=(2H/\lambda^2)w_1)$ is equal to the shell thickness. The parameter ϵ can now be regarded as a measure of the contribution of W_1 to the vertical deflection in the post-buckled state. The definition of ϵ can be made quite precise by the introduction of an orthogonality condition between (w_1,f_1) and the succeeding functions (w_n,f_n) in (22). If p_c denotes the critical load it is evident that $\epsilon \to 0$ as $p \to p_c$. It will be assumed that (22) is asymptotically valid for $\epsilon \ll 1$. Using the principle of virtual work, and assuming that θ and Φ can be expanded in powers of $(p - p_c)$, it can be shown that (22) implies a relation of the form

$$p/p_c = 1 + a\epsilon + b\epsilon^2 + \ldots \quad (23)$$

The coefficients a and b are independent of the load and can be expressed in terms of integrals over the shell base plane involving (θ,Φ), (w_1,f_1) and (w_2,f_2). Using the fact that the circumferential dependence of (w_1,f_1) is $\cos n\Theta$ it is easily shown that $a = 0$. This means that the sign of b determines whether the load initially increases or decreases after bifurcation. By substituting (22) in (1–6) it can be shown that (w_2,f_2) must be of the form‡

$$\begin{Bmatrix} -\int^x \beta(x)dx \\ \int^x \psi(x)dx \end{Bmatrix} + \begin{Bmatrix} \omega(x) \\ \chi(x) \end{Bmatrix} \cos 2n\Theta$$

The functions (β,ψ) and (ω,χ) satisfy the equations

$$(x\beta')' - (1/x + \Phi_c)\beta + (x - \theta_c)\psi = g_1(x) \quad (24)$$

$$(x\psi')' - (1/x)\psi - (x - \theta_c)\beta = g_2(x) \quad (25)$$

$$\beta(\lambda) = 0 \quad (26)$$

$$\lambda\psi'(\lambda) - \nu\psi(\lambda) = 0 \quad (27)$$

and

$$L_{2n}{}^2(\omega) - L_{2n}(\chi) + \left(\frac{1}{x}\chi' - \frac{4n^2}{x^2}\chi\right)\theta_c' - \frac{1}{x}\omega''\Phi_c + \frac{1}{x}\chi''\theta_c - \left(\frac{1}{x}\omega' - \frac{4n^2}{x^2}\omega\right)\Phi_c' = h_1(x) \quad (28)$$

$$L_{2n}{}^2(\chi) + L_{2n}(\omega) - \left(\frac{1}{x}\omega' - \frac{4n^2}{x^2}\omega\right)\theta_c' - \frac{1}{x}\omega''\theta_c = h_2(x) \quad (29)$$

$$\omega(\lambda) = \omega'(\lambda) = 0 \quad (30, 31)$$

$$\chi''(\lambda) - (\nu/\lambda)\chi'(\lambda) + (4n^2\nu/\lambda^2)\chi(\lambda) = 0 \quad (32)$$

$$\lambda\chi'''(\lambda) - \frac{1}{\lambda}[1 - \nu + 4(2+\nu)n^2]\chi'(\lambda) + \frac{12n^2}{\lambda^2}\chi(\lambda) = 0 \quad (33)$$

where (θ_c,Φ_c) is the axisymmetric solution evaluated at p_c and

$$g_1 = \tfrac{1}{2}[n^2(w_{1n}f_{1n}/x)' - w'_{1n}f'_{1n}]$$

$$g_2 = \tfrac{1}{4}[n^2(w_{1n}{}^2/x)' - (w_{1n}')^2]$$

‡ The orthogonality condition mentioned above precludes the inclusion of an arbitrary multiple of the buckling mode in (w_2,f_2).

$$h_1 = \frac{1}{2}\left[\left(\frac{1}{x}f'_{1n} - \frac{n^2}{x^2}f_{1n}\right)w''_{1n} + \left(\frac{1}{x}w'_{1n} - \frac{n^2}{x^2}w_{1n}\right)f''_{1n} + 2n^2\left(\frac{1}{x}f'_{1n} - \frac{1}{x^2}f_{1n}\right)\left(\frac{1}{x}w'_{1n} - \frac{1}{x^2}w_{1n}\right)\right]$$

$$h_2 = -\frac{1}{2}\left[n^2\left(\frac{1}{x}w'_{1n} - \frac{1}{x^2}w_{1n}\right)^2 + \left(\frac{1}{x}w'_{1n} - \frac{n^2}{x^2}w_{1n}\right)w''_{1n}\right]$$

It was shown in Ref. 3 that

$$b = -(1/p_c)\left\{\int_0^\lambda \left[\beta g_1 - \psi g_2 - \frac{1}{2}x(\omega h_1 - \chi h_2)\right]dx \Big/ \int_0^\lambda \left[\left(\frac{\partial\theta}{\partial p}\right)_c g_1 - \left(\frac{\partial\Phi}{\partial p}\right)_c g_2\right]dx\right\}$$

The denominator of this expression may be transformed by substituting for g_1 and g_2 from (24) and (25), integrating by parts, and using the equations obtained from (7–13) by differentiation with respect to p. One then obtains the formula

$$b = \int_0^\lambda \left[\beta g_1 - \psi g_2 - \frac{1}{2}x(\omega h_1 - \chi h_2)\right]dx \Big/ 2p_c\bar{\lambda}^2 \int_0^\lambda y\beta dx \tag{34}$$

where y is defined by (11).

An expression for the initial slope of the bifurcation branch of the equilibrium path on a load-deflection plot can be derived from the preceding results. Let S_0 be the rate of change of p with respect to $\overline{W}/t$ at p_c on the axisymmetric path, and S the same quantity on the bifurcation path. From (14)

$$\frac{1}{S_0} = \frac{1}{[12(1-\nu^2)]^{1/2}}\int_0^\lambda y\left(\frac{\partial\theta}{\partial p}\right)_c dx$$

and from (22) and (23)

$$S = S_0/(1+\gamma)$$

where

$$\gamma = \frac{S_0}{bp_c[12(1-\nu^2)]^{1/2}}\int_0^\lambda y\beta dx$$

A convenient measure of the postbuckling load-deflection variation is provided by the quantity

$$\begin{aligned}\alpha &= (2/\pi)\arctan[S/(S_0 - S)] \\ &= (2/\pi)\arctan(1/\gamma)\end{aligned} \tag{35}$$

which can vary between $+1$ and -1, is positive for increasing load, and negative for decreasing load (see Fig. 2). Values of α between -1 and $-\frac{1}{2}$ correspond to a backward sloping postbuckling load-deflection curve, with decreasing load.

Now suppose the cap has an initial stress-free geometric imperfection. It is reasonable to presume that the buckling behavior will be most sensitive to an imperfection in the shape of the buckling mode of the perfect shell. One might then inquire as to whether it is possible for the load-deflection curve of the imperfect structure to have a local maximum at a load p_s below the classical critical load p_c. Let the vertical component of the imperfection displacement be given by $\bar{\epsilon}\overline{W}_1$ where $\bar{\epsilon} \ll 1$. A modification of the analysis described previously, which again uses the principle of virtual work as its major tool, leads to the conclusion that p_s must satisfy an equation of the form

$$(1 - p_s/p_c)^{3/2} = C[\bar{\epsilon}(-b)^{1/2}/p_c]$$

where C is a real number and b is given by (34). Only in the case $b < 0$ does this equation admit a real-valued solution $p_s < p_c$. Thus only when the load decreases after buckling for the perfect structure will the buckling behavior be expected to be sensitive to an initial geometric imperfection.

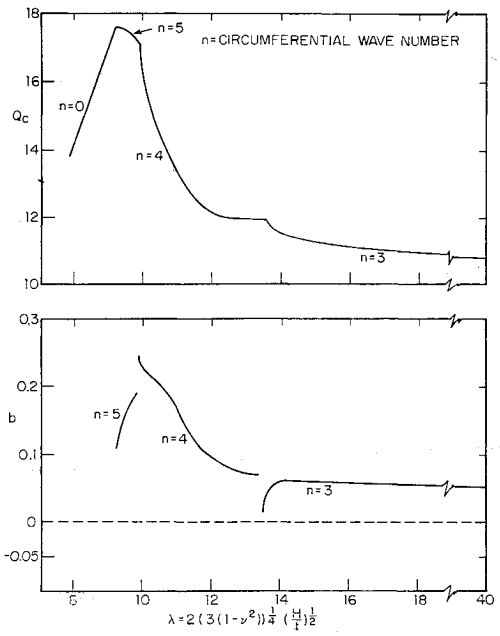

Fig. 3 Buckling and postbuckling of clamped spherical cap under concentrated load.

Numerical Procedure and Results

The details of the numerical methods used to solve the axisymmetric prebuckling problem (7–13), the buckling problem (16–21), and the postbuckling equations (24–27) and (28–33) were described in Ref. 3 and will not be repeated here. The nonlinear axisymmetric problem was solved by Newton's method[13,14] in which the direct solution of the nonlinear system is replaced by the solution of a sequence of linear correctional equations. These equations, as well as those of the buckling and postbuckling problems, were solved by central differencing, and the application of Potters' algorithm.[15] The integrals in the formulas for b and γ were evaluated by Simpson's rule. Poisson's ratio was taken as $\frac{1}{3}$ in all calculations.

To serve as background to the present study, the results of Ref. 3 for the case of a concentrated apex load are reproduced in Fig. 3. Here the nondimensional critical load

$$Q_c = (6/\pi)(1-\nu^2)PR/Et^3 \tag{36}$$

(where P is the load) is plotted against the shell geometry parameter λ, as is the postbuckling coefficient b wherever nonaxisymmetric buckling occurs. As λ increases, the number n of circumferential waves changes from zero (for axisymmetric snapping) to 5 to 4 to 3, and, as indicated by the positive values of b, the initial postbuckling behavior for $n \neq 0$ is characterized by increasing load.

Attention was first focused in the present work on the geometry characterized by $\lambda = 12$, and a study was made of the effect of increasing the size of the circle over which the loading is uniformly spread. The results are shown in Fig. 4. The top curve shows the critical load as a function of $\bar{\lambda}$, the parameter measuring the extent of the loaded area; $\bar{\lambda}$ varies from zero to λ as the loading changes from a concentrated force at the apex to a uniform load over the entire shell. In this diagram the nondimensional load parameter Q_c, now given by Eq. (36) with $P = (\pi\bar{r}^2)q$, is plotted for $\bar{\lambda} \leq 2$; however, for $\bar{\lambda} > 2$ the pressure parameter

$$p_c = q/q_0 \tag{37}$$

where $q_0 = 2E/[3(1-\nu^2)]\,(t/R)^2$ is the classical buckling pressure for a complete sphere, was used.

The middle portion of Fig. 4 gives the values of the postbuckling coefficient b associated with asymmetric bifurca-

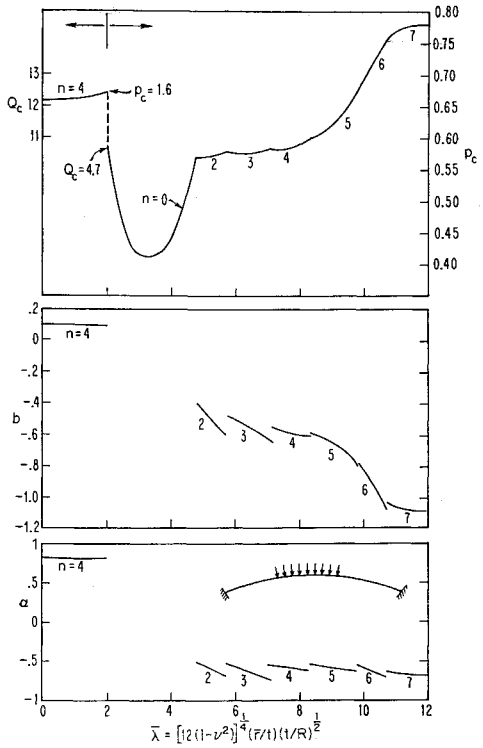

Fig. 4 Buckling and postbuckling behavior of a clamped spherical cap under distributed load for $\lambda = 12$.

tion buckling. Finally, the bottom part of the figure shows the postbuckling stiffness parameter α, the significance of which has been illustrated in Fig. 2.

The buckling and initial postbuckling behavior shown in Fig. 4 may be described as follows. For $\bar{\lambda} \leq 2$ the situation is very much the same as for the concentrated load case corresponding to $\bar{\lambda} = 0$. Asymmetric bifurcation occurs before axisymmetric snap-buckling, and b is positive. For $2 < \bar{\gamma} < 4.8$ a local maximum on the axisymmetric load-deflection curve appears before the lowest bifurcation load. This transition in the mode of buckling at $\bar{\lambda} = 2$ is marked by a discontinuous drop in the critical load (thus the jump in the curve is not just due to the change in the vertical scale). For $\bar{\lambda} > 4.8$ bifurcation again occurs before axisymmetric snap-buckling, but now b is negative. As $\bar{\lambda}$ is increased the critical wave number proceeds through a sequence of values starting with $n = 2$. The most important fact to be extracted from these curves is that for $\bar{\lambda} > 2$ buckling will be accompanied by a loss of load carrying capacity, and at least for $\bar{\lambda} > 4.8$, the buckling behavior will be imperfection-sensitive; that is, a drop in the critical load would be expected to result from the presence of an initial imperfection. From the definition of $\bar{\lambda}$ one can say that a loss of load carrying capacity at buckling will occur if

$$\bar{r}/t > 2/[12(1 - \nu^2)]^{1/4}(R/t)^{1/2} \tag{38}$$

There is, of course, an additional dependence on ν which enters through the boundary conditions (10, 20, 21, 27, 32, and 33), in which ν has been set equal to $\frac{1}{3}$. For $\nu = \frac{1}{3}$, (38) is well approximated by

$$\bar{r} > (Rt)^{1/2} \tag{39}$$

The results shown for α at the bottom of Fig. 4 have the same trends, of course, as those for b, but reveal the additional interesting fact that for $\bar{\lambda} > 4.8$ the initial postbuckling load-deflection relation always involves decreasing deflection as well as decreasing load.

Calculations were also made for the limiting case of $\lambda = \infty$, with the results shown in Fig. 5. (These calculations were actually made for a value of λ sufficiently large that, when doubled, led to no appreciable change in the results.) Except that n equals 3 rather than 4 in the imperfection-insensitive range at small $\bar{\lambda}$, the results are qualitatively similar to those for $\lambda = 12$. In fact, they are so nearly the same in the range $2 < \bar{\lambda} < 8$, that it is likely that the buckling pressures found for $\lambda = \infty$ hold fairly well for $\lambda > 12$ and $2 < \bar{\lambda} < (\lambda\text{-}4)$. (That is, it would appear that the buckling behavior for $\lambda > 12$ is not affected much by the clamped boundary as long as it is more than 4 λ-units from the edge of the loaded region.) Also shown are asymptotic results for p_c and b, found as described in the Appendix, for $\bar{\lambda} \to \infty$, with $\bar{\lambda}/\lambda$ kept equal to zero.

Figure 6 shows, for $\lambda = \infty$, three examples of axisymmetric load deflection curves which may help to clarify the nature of the transition at $\bar{\lambda} = 2$. The $\bar{\lambda} = 2$ curve illustrates the situation which prevails for $\bar{\lambda} \leq 2$. The curve has a pronounced flattening in the neighborhood of $p = 0.6$, but remains monotonically increasing and eventually encounters a point of bifurcation. The behavior in the region in which axisymmetric snap-buckling prevails is exemplified by the curve for $\bar{\lambda} = 4$. The flattened region has developed into a well-defined maximum. For $\bar{\lambda} = 6$ the maximum is still present, but a bifurcation point has appeared at a smaller load.

Figure 7 shows how, for $\lambda = \infty$, several mode shapes associated with asymmetric bifurcation vary with the nondimensional radial coordinate x. Note that the peak value for a very localized loading ($\bar{\lambda} = 1$) is further from the apex than that for $\bar{\lambda} = 5$. As $\bar{\lambda}$ continues to increase, however, the buckling mode appears to peak in the vicinity of the boundary between the loaded and unloaded regions, and decays rapidly in both directions; this was verified for $\bar{\lambda} \to \infty$ ($\bar{\lambda}/\lambda = 0$) by the asymptotic study of the Appendix. In contrast, the buckling mode for large λ with a concentrated load at the apex has a boundary layer near the apex, whereas the large-λ buckling mode of Ref. 1 for uniform loading has a boundary layer near the clamped edge.

Finally, it was thought desirable to supplement Huang's investigation[1] by studying the initial postbuckling behavior of clamped spherical caps under uniform pressure over the full range of λ; the results are shown in Fig. 8. As suspected, the postbuckling coefficient b is always negative; indeed, the fact that b is of order -1 suggests that the clamped cap is just about as imperfection sensitive as the complete spherical shell under uniform pressure.[16] As shown in Fig. 8, asympto-

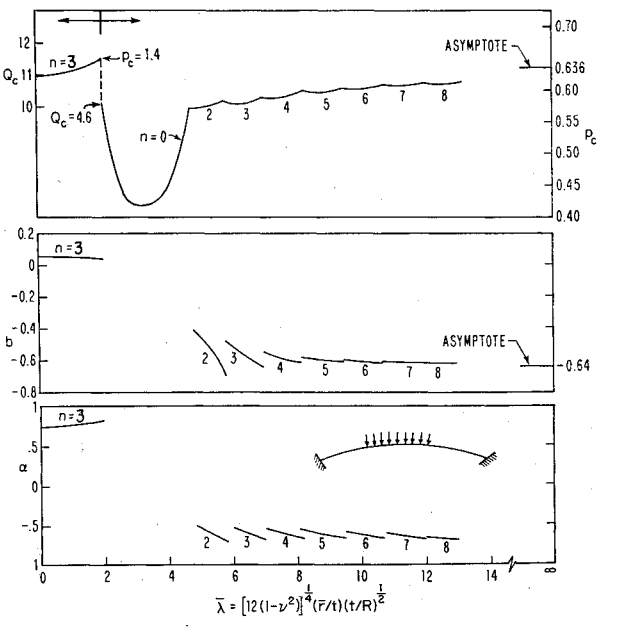

Fig. 5 Buckling and postbuckling behavior of a spherical cap under distributed load in the limit as $\lambda \to \infty$.

tic results for $\lambda \to \infty$ were found for both p_c and b; for reasons discussed in the Appendix, the asymptotic value obtained for p_c is about 7% smaller than that calculated by Huang.

Appendix: Asymptotic Analysis

In this Appendix the procedure used to obtain the asymptotic values of p_c and b shown on Figs. 8 and 5 is described.

Uniform Pressure Case

Huang[1] computed the limiting value of p_c as λ approaches infinity for a clamped spherical cap under uniform pressure. A summary of his work will be given because it provides the basis for the asymptotic calculation of b. The fundamental step in the analysis is the recognition that as λ becomes large the bending of the shell is confined to a narrow region adjacent to the clamped edge. Outside this region the membrane state $\theta = 0$, $\Phi = -2px$ accurately describes the axisymmetric prebuckling solution. The only trouble with this solution is that it does not satisfy the boundary conditions at $x = \lambda$. Huang proceeded to define a new variable $\bar{\Phi}$ by writing $\Phi = -2px + \bar{\Phi}$. Substituting for Φ in (7) and (8) gives

$$(x\theta')' - \theta/x + x\bar{\Phi} = -2px\theta + \theta\bar{\Phi}$$

$$(x\bar{\Phi}')' - \bar{\Phi}/x - x\theta = -\tfrac{1}{2}\theta^2$$

If it is assumed that θ, $\bar{\Phi}$ and their derivatives remain bounded as $\lambda \to \infty$ it is evident that these equations may, in the boundary layer where x is large, be replaced by

$$\theta'' + 2p\theta + \bar{\Phi} = 0 \tag{40}$$

$$\bar{\Phi}'' - \theta = 0 \tag{41}$$

Similarly the boundary conditions (9) and (10) become

$$\theta(\lambda) = 0 \tag{42}$$

$$\bar{\Phi}'(\lambda) = 2(1 - \nu)p \tag{43}$$

Huang solved (40–43) subject to the necessary condition that θ and $\bar{\Phi}$ vanish exponentially as x moves away from the boundary. He obtained

$$\theta = [2(2)^{1/2}(1-\nu)p/(1+p)^{1/2}]e^{-[(1-p)/2]^{1/2}\eta}\sin[(1+p)/2]^{1/2}\eta$$

$$\bar{\Phi} = [2(2)^{1/2}(1-\nu)p/(1+p)^{1/2}]e^{-[(1-p)/2]^{1/2}\eta}\{(1-p^2)^{1/2}\times \cos[(1+p)/2]^{1/2}\eta - p\sin[(1+p)/2]^{1/2}\eta\}$$

where $\eta = \lambda - x$.

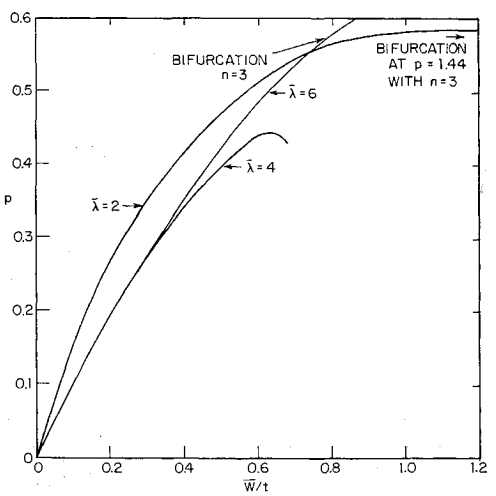

Fig. 6 Axisymmetric load deflection curves for a spherical cap under distributed load in the limit as $\lambda \to \infty$.

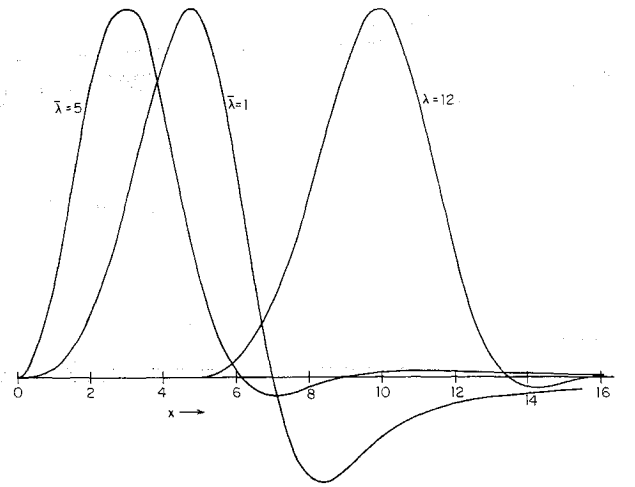

Fig. 7 Buckling mode shapes for spherical cap under distributed load ($\lambda = \infty$).

Proceeding to the buckling problem Huang observed, from the exact numerical results for large finite λ, that the functions w_{1n} and f_{1n} are essentially zero outside an interval $\lambda - \delta < x < \lambda$ where δ is independent of λ. As $\lambda \to \infty$ Eqs. (16–21) can be replaced within this boundary layer by

$$w'''' - 2\sigma w'' + \sigma^2 w - f'' + \sigma(1+\theta')f + 2pw'' - \sigma(2p + \bar{\Phi}')w = 0 \tag{44}$$

$$f'''' - 2\sigma f'' + \sigma^2 f + w'' - \sigma(1+\theta')w = 0 \tag{45}$$

$$w(0) = w'(0) = 0 \tag{46, 47}$$

$$f''(0) + \nu\sigma f(0) = 0 \tag{48}$$

$$f'''(0) - 2(1+\nu)\sigma f'(0) = 0 \tag{49}$$

where η is now the independent variable and

$$\sigma = \lim_{\lambda\to\infty}\left(\frac{n}{\lambda}\right)^2$$

(The subscripts on w_{1n} and f_{1n} have been dropped for simplicity.) Equation (44) differs from that given by Huang by the appearance of $\bar{\Phi}'$ in the last term. It can be seen from (43) that $\bar{\Phi}'$ cannot be neglected relative to $2p$. The asymptotic value of p_c is the smallest eigenvalue of (44–49) for any σ. It was found numerically to be 0.810, and it occurred for $\sigma = 0.728$. The 7% difference between this value of p_c and

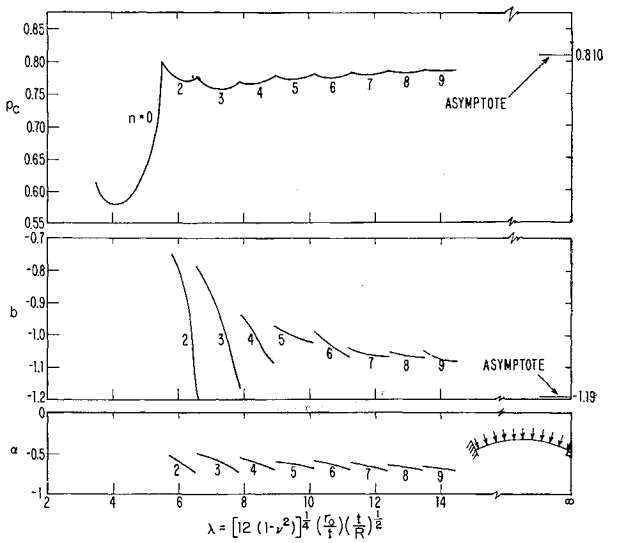

Fig. 8 Buckling and postbuckling behavior of a clamped spherical cap under uniform pressure.

that computed by Huang is due to the discrepancy in (44) just discussed.

The preceding method of analysis can be extended to the equations describing the behavior of the functions β, ψ, ω, and χ which enter into the formula for b. The numerical results for large finite λ show that these functions also approach zero outside the boundary layer. This is only reasonable since their governing equations are driven by the buckling mode. In the limit of large λ, then, (24–33) can be replaced by

$$\beta'' + 2p_c\beta + \psi = -\tfrac{1}{2}\sigma(wf)' \tag{50}$$

$$\psi'' - \beta = -\tfrac{1}{2}\sigma ww' \tag{51}$$

$$\beta(0) = \psi'(0) = 0 \tag{52, 53}$$

and

$$\omega'''' - 8\sigma\omega'' + 16\sigma^2\omega - \chi'' + 4\sigma(1 + \theta_c')\chi + 2p_c\omega'' - 4\sigma(2p_c + \bar{\Phi}_c')\omega = \tfrac{1}{2}\sigma(2w'f' - w''f + wf'') \tag{54}$$

$$\chi'''' - 8\sigma\chi'' + 16\sigma^2\chi + \omega'' - 4\sigma(1 + \theta_c')\omega = -\tfrac{1}{2}\sigma[(w')^2 - ww''] \tag{55}$$

$$\omega(0) = \omega'(0) = 0 \tag{56, 57}$$

$$\chi''(0) + 4\sigma\nu\chi(0) = 0 \tag{58}$$

$$\chi'''(0) - 4\sigma(2 + \nu)\chi'(0) = 0 \tag{59}$$

where σ and p_c are 0.728 and 0.810, respectively. Both the numerator and denominator in formula (34) for b increase without bound as $\lambda \to \infty$, but it is not difficult to show that

$$\lim_{\lambda\to\infty} b = \frac{1}{p_c}\frac{\int_0^\infty \left[\beta\bar{g}_1 - \psi\bar{g}_2 - \frac{1}{2}(\omega\bar{h}_1 - \chi\bar{h}_2)\right]d\eta}{\int_0^\infty \left\{2\beta\theta_c + \frac{1}{2}[\sigma w^2 + (w')^2]\right\}d\eta - 2(1-\nu)\psi(0)} \tag{60}$$

where $\bar{g}_1$, $\bar{g}_2$, $\bar{h}_1$, and $\bar{h}_2$ are the right-hand sides of (50, 51, 54 and 55). For numerical evaluation the upper limit on the integrals in (60) may, of course, be replaced by the actual boundary-layer width. The result obtained by numerical solution of (50–59) and evaluation of (60) is $b = -1.19$.

Intermediate Load Distribution

A similar analysis was used to compute the asymptotic values of p_c and b shown on Fig. 5. These results were obtained in the limit as λ and $\bar{\lambda}$ approach infinity, with $\bar{\lambda}/\lambda = 0$. The bending is then confined to a narrow region near the boundary between the loaded and unloaded portions of the shell. Outside this region the axisymmetric solution in the loaded section is accurately given by $\theta = 0$, $\Phi = -2px$, and in the unloaded section by $\theta = 0$, $\Phi = -2p\bar{\lambda}^2/x$. The only failing of the membrane solution described above is that Φ' is discontinuous at $x = \bar{\lambda}$, which implies a discontinuity in the hoop strain. To remedy this we will seek a boundary-layer correction in the neighborhood of $x = \bar{\lambda}$. Let

$$\Phi = -2px\,\bar{y}(x) + \bar{\Phi} \tag{61}$$

where

$$\bar{y}(x) = \begin{cases} 1, & x < \bar{\lambda} \\ \bar{\lambda}^2/x^2, & x > \bar{\lambda} \end{cases}$$

Substituting for Φ in Eqs. (7) and (8) gives

$$(x\theta')' - \theta/x + x\bar{\Phi} = -2px\,\bar{y}\theta + \theta\bar{\Phi}$$

$$(x\bar{\Phi}')' - \bar{\Phi}/x - x\theta = -\tfrac{1}{2}\theta^2$$

In the limit of large $\bar{\lambda}$ these equations may, in the neighborhood of $x = \bar{\lambda}$, be replaced by

$$\theta'' + \bar{\Phi} = -2p\theta \tag{62}$$

$$\bar{\Phi}'' - \theta = 0 \tag{63}$$

With the coordinate change $x = \xi + \bar{\lambda}$ the problem may be stated as that of finding a solution of (62) and (63) which vanishes exponentially as $\xi \to \pm\infty$. In addition we require continuity of θ, θ', and $\bar{\Phi}$ at $\xi = 0$ along with the jump condition

$$\bar{\Phi}'(0+) - \bar{\Phi}'(0-) = -4p$$

which is the jump required to make Φ' continuous. These conditions lead to the solution

$$\theta = [p(2)^{1/2}/(1-p)^{1/2}]\, e^{-[(1-p)/2]^{1/2}|\xi|}\{\cos[(1+p)/2]^{1/2}\,\xi + [(1-p)/(1+p)]^{1/2}\sin[(1+p)/2]^{1/2}\,|\xi|\}$$

$$\bar{\Phi} = [p(1-2p)(2)^{1/2}/(1-p)^{1/2}]\, e^{-[(1-p)/2]^{1/2}|\xi|}\{\cos[(1+p)/2]^{1/2}\,\xi - [(1+2p)/(1-2p)]\,[(1-p)/(1+p)]^{1/2}\sin[(1+p)/2]^{1/2}\,|\xi|\}$$

The exact numerical results for large $\bar{\lambda}$ show that the functions w_{1n} and f_{1n} are essentially zero outside an interval $\bar{\lambda} - \delta < x < \bar{\lambda} + \delta$, where δ is independent of $\bar{\lambda}$. Thus in the limit as $\bar{\lambda} \to \infty$ Eqs. (16) and (17) may be replaced by

$$w'''' - 2\bar{\sigma}w'' + \bar{\sigma}^2 w - f'' + \bar{\sigma}(1-\theta')f + 2pw'' + \bar{\sigma}w[2p(\xi/|\xi|) + \bar{\Phi}'] = 0 \tag{64}$$

$$f'''' - 2\bar{\sigma}f'' + \bar{\sigma}^2 f + w'' - \bar{\sigma}(1-\theta')w = 0 \tag{65}$$

where

$$\bar{\sigma} = \lim_{\bar{\lambda}\to\infty}\left(\frac{n}{\bar{\lambda}}\right)^2$$

The description of this eigenvalue problem was completed by the imposition of appropriate continuity conditions on w, f, and their derivatives at $\xi = 0$. The minimum value of p_c was found numerically to be 0.636 and it occurs for $\bar{\sigma} = 0.610$. The functions β, ψ, ω, and χ are also practically zero outside the $(\bar{\lambda} - \delta, \bar{\lambda} + \delta)$ interval for large $\bar{\lambda}$; in the limit as $\bar{\lambda} \to \infty$ their governing differential equations may thus be replaced by

$$\beta'' + 2p_c\beta + \psi = \tfrac{1}{2}\bar{\sigma}(wf)' \tag{66}$$

$$\psi'' - \beta = \bar{\sigma}\tfrac{1}{2}ww' \tag{67}$$

and

$$\omega'''' - 8\bar{\sigma}\omega'' + 16\bar{\sigma}^2\omega - \chi'' + 4\bar{\sigma}(1-\theta_c')\chi + 2p_c\omega'' + 4\bar{\sigma}\omega\left(2p_c\frac{\xi}{|\xi|} + \bar{\Phi}_c'\right) = \bar{\sigma}\left(w'f' - \frac{w''f + wf''}{2}\right) \tag{68}$$

$$\chi'''' - 8\bar{\sigma}\chi'' + 16\bar{\sigma}^2\chi + \omega'' - 4\bar{\sigma}(1-\theta_c')\omega = -\tfrac{1}{2}\bar{\sigma}[(w')^2 - ww''] \tag{69}$$

Finally, it can be shown that

$$\lim_{\bar{\lambda}\to\infty} b = \frac{1}{p_c}\frac{\int_{-\infty}^{\infty}\left[\beta\bar{g}_1 - \psi\bar{g}_2 - \frac{1}{2}(\omega\bar{h}_1 - \chi\bar{h}_2)\right]d\xi}{\int_{-\infty}^{\infty}\left\{2\beta\theta_c - \frac{1}{2}\left[\bar{\sigma}w^2\frac{\xi}{|\xi|} - (w')^2\right]\right\}d\xi - 4\psi(0)} \tag{70}$$

where $\bar{g}_1$, $\bar{g}_2$, $\bar{h}_1$, and $\bar{h}_2$ are the right-hand sides of (66–69), respectively. These equations were solved numerically subject to appropriate continuity conditions at $\xi = 0$. The asymptotic value of b was then evaluated from (70) with the upper and lower limits on the integrals replaced by $\pm\delta$, respectively. The result, shown on Fig. 5, is $b = -0.645$.

References

[1] Huang, N. C., "Unsymmetrical Buckling of Thin Shallow Spherical Shells," *Journal of Applied Mechanics*, Vol. 31, 1964, p. 447.

[2] Bushnell, D., "Bifurcation Phenomena in Spherical Shells under Concentrated and Ring Loads," *AIAA Journal*, Vol. 5, No. 11, Nov. 1967, pp. 2034-2040.

[3] Fitch, J., "The Buckling and Post-Buckling Behavior of Spherical Caps Under Concentrated Load," *International Journal of Solids and Structures*, Vol. 4, 1968, pp. 421-466.

[4] Penning, F. A. and Thurston, G. A., "The Stability of Shallow Spherical Shells Under Concentrated Load," Contract Rept. 265, 1965, NASA.

[5] Penning, F. A., "Nonaxisymmetric Behavior of Shallow Shells Loaded at the Apex," *Journal of Applied Mechanics*, Vol. 33, 1966, p. 699.

[6] Evan-Iwanowski, R. M., Cheng, H. S., and Loo, T. C., "Experimental Investigations on Deformations and Stability of Spherical Shells Subjected to Concentrated Loads at the Apex," *Proceedings of 4th U.S. National Congress of Applied Mechanics*, 1962, p. 563.

[7] Kaplan, A. and Fung, Y. C., "A Nonlinear Theory of Bending and Buckling of Thin Elastic Shallow Spherical Shells," TN 3212, Aug. 1954, NACA.

[8] Homewood, R. H., Brine, A. C., and Johnson, A. E., Jr., "Experimental Investigation of the Buckling Instability of Monocoque Shells," *Proceedings of the Society of Experimental Stress Analysis*, Vol. 18, 1961, p. 88.

[9] Krenzke, M. A. and Kiernan, T. J., "Elastic Stability of Near Perfect Shallow Spherical Shells," *AIAA Journal*, Vol. 1, No. 12, Dec. 1963, p. 3855.

[10] Marguerre, K., "Zur Theorie der gekrümmten Platte grosser Formanderung," *Proceedings of 5th International Congress of Applied Mechanics*, 1938, p. 93.

[11] Koiter, W. T., "On the Stability of Elastic Equilibrium" (in Dutch), Thesis, Delft, H. J. Paris, Amsterdam, 1945.

[12] Koiter, W. T., "Elastic Stability and Post-Buckling Behavior," *Proceedings of Symposium on Nonlinear Problems*, edited by R. E. Langer, University of Wisconsin Press, 1963, p. 257.

[13] Mescall, J. F., "On the Numerical Analysis of the Nonlinear Axisymmetric Equations for Shells of Revolution," TR 64-20, 1964, U.S. Army Materials Research Agency.

[14] Thurston, G. A., "Newton's Method Applied to Problems in Nonlinear Mechanics," *Journal of Applied Mechanics*, Vol. 32, 1965, p. 383.

[15] Potters, M. L., "A Matrix Method for the Solution of a Second Order Difference Equation in Two Variables," Rept. MR19, Mathematich Centrum, Amsterdam, 1955.

[16] Hutchinson, J. W., "Imperfection Sensitivity of Externally Pressurized Spherical Shells," *Journal of Applied Mechanics*, March 1967, pp. 49-55.

APRIL 1970 AIAA JOURNAL VOL. 8, NO. 4

Vibrations of Pressurized Orthotropic Cylindrical Membranes

CLIVE L. DYM*

Bell Aerosystems Company, Niagara Falls, N. Y.

This paper presents the analysis of the free and forced vibrations of pressurized orthotropic cylindrical membrane shells. The following points are brought out. 1) The response of the shell is very highly dependent on the internal pressure, and on the relative magnitude of the applied pressure loading as compared to the internal pressure. In fact, it is clearly demonstrated that when the two pressures are of the same order of magnitude, a linearized analysis is not sufficient to discuss the complete behavior. 2) The behavior of the shell is also very significantly affected by the values of the various elastic constants. The ratio of the circumferential stiffness to the axial stiffness was found to be a particularly important parameter, with somewhat less importance being attached to the relative magnitude of the inplane shear modulus. 3) Finally, the simplification of the analysis by the deletion of the inplane inertia terms makes little difference in the results of the forced vibration analysis. This is a particularly important simplification to recognize if a full nonlinear analysis is to be carried out.

Nomenclature

b,d,α_1	= dimensions defined in Fig. 8
C_{ij},G_{12}	= orthotropic material constants
h	= thickness of cylinders
K	= dimensionless frequency parameter
L	= length of cylinder
n,λ	= circumferential and axial wave numbers
p	= initial internal pressure
p_x,p_y,p_z	= applied surface tractions
q_{mn}	= mode participation factor
R	= radius of cylinder
t_x,t_y,t_{xy}	= dimensionless stress components
t_{x0},t_{y0},t_{xy0}	= initial stress state
$\tilde{t}_x,\tilde{t}_y,\tilde{t}_{xy}$	= stress perturbations
U_{mn},V_{mn},W_{mn}	= modal displacements
u,v,w	= dimensionless displacements
u^*,v^*,w^*	= axial, circumferential, and inward normal displacements
u_0,v_0,w_0	= initial displacements
$\tilde{u},\tilde{v},\tilde{w}$	= displacement perturbations
x,y	= axial and circumferential coordinates
α,β,γ	= dimensionless material constants
$\epsilon_x,\epsilon_y,\gamma_{xy}$	= strain components
ξ,φ	= dimensionless coordinates
ρ	= mass density
τ	= dimensionless time

Received January 16, 1969; revision received October 30, 1969. The author is grateful to W. Garth, N. Markwart, and G. Worner of the Electronic Data Processing Group of the Bell Aerosystems Company for the computation of the numerical results presented here, to J. W. Leonard (SUNY-Buffalo) for useful discussions, and to the reviewers for helpful suggestions.

* Research Scientist. Member AIAA.

Introduction

THIS work presents a study of the dynamic response of a pressurized orthotropic cylindrical membrane in both free and forced vibration configurations. The effects of internal pressurization, inplane inertia terms, and variations in the elastic constants will be examined.